Identification of the fragment of the 1-methylpyrene cation by mid-IR spectroscopy

Pavol Jusko[a,b], Aude Simon[c], Gabi Wenzel[a], Sandra Brünken[d,b], Stephan Schlemmer[b], Christine Joblin[a,*]

[a] *Institut de Recherche en Astrophysique et Planétologie (IRAP), Université de Toulouse (UPS), CNRS, CNES, 9 Av. du Colonel Roche, 31028 Toulouse Cedex 4, France*
[b] *I. Physikalisches Institut, Universität zu Köln, Zülpicher Str. 77, 50937 Köln, Germany*
[c] *Laboratoire de Chimie et Physique Quantiques LCPQ/IRSAMC, Université de Toulouse (UPS) and CNRS, 118 Route de Narbonne, 31062 Toulouse, France*
[d] *Radboud University, Institute for Molecules and Materials, FELIX Laboratory, Toernooiveld 7c, 6525 ED Nijmegen, The Netherlands*

Abstract

The fragment of the 1-methylpyrene cation, $C_{17}H_{11}^+$, is expected to exist in two isomeric forms, 1-pyrenemethylium $PyrCH_2^+$ and the tropylium containing species $PyrC_7^+$. We measured the infrared (IR) action spectrum of cold $C_{17}H_{11}^+$ tagged with Ne using a cryogenic ion trap instrument coupled to the FELIX laser. Comparison of the experimental data with density functional theory calculations allows us to identify the $PyrCH_2^+$ isomer in our experiments. The IR Multi-Photon Dissociation spectrum was also recorded following the C_2H_2 loss channel. Its analysis suggests combined effects of anharmonicity and isomerisation while heating the trapped ions, as shown by molecular dynamics simulations.

Keywords: PAH, 22 pole cryogenic ion trap, Ne tagging spectroscopy, molecular dynamics simulations

1. Introduction

The photoproduct of the 1-methylpyrene cation, $C_{17}H_{11}^+$, has been pointed out in matrix-isolation studies as a candidate of interest to account for some of the diffuse interstellar bands including the strongest one at 4428 Å [1]. This has motivated experimental studies using the ion trap setup PIRENEA in which CH_3-$C_{16}H_9^+$ ions were trapped, irradiated by UV-VIS photons and its photofragment, $C_{17}H_{11}^+$, could be isolated. First multi-photon dissociation (MPD) spectra were obtained in order to reveal the structure of these ions [2]. Rapacioli et al. performed extensive calculations on the possible isomers and isomerisation pathways [3]. These studies have shown that both the 1-pyrenemethylium isomer,

*christine.joblin@irap.omp.eu

$PyrCH_2^+$, and the isomer containing a tropylium cycle, $PyrC_7^+$ (see Figure 1), could be present under the experimental conditions used in [2]. Both isomers were found to be quasi degenerate (cf. Table 3 in [3]). In addition, theoretical calculations showed several isomerisation pathways with barrier heights in the range of $3.5 - 4.0$ eV [3]. This, together with the fact that both isomers coexist at formation, could explain why the recorded bands in MPD measurements were so broad.

Infrared (IR) spectroscopy is an obvious technique to assign absorption bands to the $PyrCH_2^+$ and $PyrC_7^+$ species and thus to disentangle the nature of the 1-methylpyrene cation photoproduct. Similarly to the case of the electronic transitions described above, absorption of multiple photons at IR wavelengths can be used to probe IR transitions of stored ions. This technique is well-known as IRMPD spectroscopy and has been successfully applied to different types of molecules and molecular complexes including polycyclic aromatic hydrocarbons (PAHs), which are of interest for this study [4, 5]. A drawback of the technique is that it implies the heating of the trapped ions by successive IR photon absorption. As a result, anharmonic effects, which lead to modifications of the IR spectrum with internal temperature, can therefore induce strong deviations of the recorded spectra compared to linear IR absorption spectra [6]. In a case like the $PyrCH_2^+$ and $PyrC_7^+$ species, an additional complication can arise from isomerisation processes induced by the heating.

The recent development of a cryogenic trap instrument [7] at the FELIX[1] Laboratory [8] opens new perspectives for this study. Indeed, it allows to use a rare gas tagging often referred to as messenger technique which provides information on the IR spectrum of the cold ion–rare gas complex upon the absorption of a single photon. This type of spectra was earlier reported in molecular beam experiments, in particular on jet-cooled complexes of cationic naphthalene-Ar, phenanthrene-Ar and phenanthrene-Ne [9, 10]. The possibility to build and store such complexes in a cryogenic ion trap opens new perspectives [11, 12], especially to isolate and study fragments of the parent species.

In this article, we present the first IR spectrum of the Ne tagged $C_{17}H_{11}^+$ species together with the IRMPD spectrum of the bare cation. The analysis of the experimental spectra involves both static Density Functional Theory (DFT) calculations to interpret the cold IR spectrum and molecular dynamics simulations to gain insights into the hot IRMPD spectrum.

2. Methods

2.1. Experimental

The experimental spectrum has been recorded on the FELion beamline at the FELIX [8] Laboratory at the Radboud University in The Netherlands. The FELion instrument at the beamline [7] consists of a cryogenic 22-pole rf ion trap

[1] Free Electron Lasers for Infrared eXperiments, `www.ru.nl/felix`

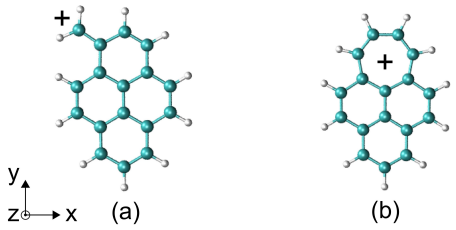

Figure 1: Topological formulas of the two isomers of $C_{17}H_{11}^+$: $PyrCH_2^+$ (a) and $PyrC_7^+$ (b).

equipped with two quadrupole mass filters allowing to mass select and analyse the ions to be studied, as well as the products created in the trap. The ions of interest were created in a storage ion source [13] via electron bombardment of the 1-methylpyrene neutral gas evaporated directly into the UHV chamber from a solid 1-methylpyrene sample (Sigma-Aldrich). The sample was heated to a temperature of 40° C in order to achieve a sufficient vapour pressure. Several thousands ions of mass-selected $C_{17}H_{11}^+$ cations ($m/z = 215$, cf. Figure S1 in the Supplementary Information (SI) for the different experimental conditions used in this work) were stored in the trap for each experimental cycle, while one of the following two spectroscopic techniques was applied:

IR Pre-Dissociation (IR-PD) of the weakly bound complex with Ne. The trap was operated at a nominal temperature of $8 - 9$ K. Upon ion injection high quantities of a Ne:He 1:2 gas mixture were introduced in order to promote ternary attachment of Ne atoms to $C_{17}H_{11}^+$ cations with a yield of only $\lesssim 1\,\%$. The depletion (single photon process) of the $C_{17}H_{11}^+ \cdot Ne$ complex was then recorded as a function of wavelength.

IR Multi-Photon Dissociation (IRMPD) of the primary ion $C_{17}H_{11}^+$. These experiments were performed at a trap temperature of about 200 K. He gas was introduced only to aid ion thermalisation and was removed prior to irradiation. The FELIX laser beam was focussed into the trap region to facilitate multi-photon absorption processes. The typical irradiation time to record the spectrum is 3 s and the major fragment corresponds to the loss of acetylene, C_2H_2 (cf. Table S1 of SI). The number of produced fragment ions at $m/z = 189$ is therefore recorded as a function of wavelength.

The FELIX laser used for the experiment delivers up to 30 mJ into the 22 pole trap in a single macropulse (about 5 μs long), at a 10 Hz repetition rate. The macropulse is composed of micropulses with energy in the 10 μJ range and with a typical length in the picosecond range. A spectral bandwidth of approximately $\sigma = 0.5\%$ was used.

2.2. Computational

Two computational approaches were used in order to i) predict the IR harmonic spectra and ii) gain insight into the dissociation dynamics during the IRMPD process.

Static DFT calculations. These were carried out in order to obtain the theoretical IR harmonic spectra of the two isomers of $C_{17}H_{11}^+$. In a recent computational study of the isomerisation reactions of $C_7H_7^+$ isomers, Kharnaior et al. [14] have concluded that the B3LYP exchange-correlation functional [15] provides good results for molecules of similar size and structure. We therefore optimised the geometries of the two isomers of $C_{17}H_{11}^+$ using the B3LYP hybrid functional in conjunction with a 6-31G(d,p) basis set [16]. These were found to be quasi degenerate at this level, with $PyrC_7^+$ being more stable than $PyrCH_2^+$ by 0.5 kJ.mol^{-1} when including zero-point energy corrections. The harmonic spectra were obtained by full diagonalization of the weighted Hessian matrix. The calculations were achieved with the Gaussian09 suite of programs [17].

Dissociation dynamics. PAHs with high enough internal energy may undergo many possible isomerisation reactions [18], among them H migrations [19], external ring openings and formation of 5-membered rings [20]. This leads to many different possible dissociation paths, and an exhaustive study of reactions mechanisms with DFT becomes very fastidious. A first insight into reaction kinetics, branching ratios and mechanisms can be obtained from molecular dynamics (MD) simulations in which the electronic structure is described on-the-fly at the Self-Consistent-Charge Density Functional based Tight Binding (SCC-DFTB) level of theory [21] (MD/SCC-DFTB), as shown in our previous work [22]. To get insight into isomerisation and dissociation mechanisms of the two isomers of $C_{17}H_{11}^+$, we ran extensive simulations following the procedure detailed in Section 2 of [22]. We also performed calculations on the regular pyrene cation as a reference system. For each molecular ion of interest, 720 simulations of 500 ps (δt = 0.1 fs) were achieved with random initial velocities in the (NVE) ensemble, at 19 eV (lowest energy necessary to observe a dissociation event) and 24 eV (to obtain significant branching ratios). The drawback of such simulations is their time limitation (less than 1 ns for a system of $\sim$30 atoms), making the use of high internal energy mandatory to observe a sufficient number of events. The calculations were achieved with the deMonNano package [23].

3. Results and Discussion

3.1. Infrared spectra

Figure 2 shows the two experimental spectra that were recorded, the IR-PD spectrum in the top panel and the IRMPD spectrum in the bottom panel. The two experimental spectra are rather different. The IR-PD spectrum exhibits several weak bands, whereas the IRMPD spectrum depicts 3 strong bands, which fall close to some of the bands in the IR-PD spectrum. Further insight into the band assignment comes from the comparison with the computed DFT harmonic IR absorption spectra of the two isomers, $PyrCH_2^+$ and $PyrC_7^+$, which are reported in the middle panel. Both isomers were found to have an ^{1}A' ground-state. All band frequencies were multiplied by a unique scaling factor of 0.975

obtained by adjusting the position of the most intense band in the calculated spectrum of $PyrCH_2^+$ at 1656 cm^{-1} to the band located at 1615 cm^{-1} in the IR-PD spectrum. This factor is in accordance with those used previously for similar systems [24]. All IR bands in the $1100 - 1670$ cm^{-1} region involve C-C stretching and in-plane C-H bending modes (a' symmetry; Figures S2 and S3 in the SI for more information on the assignment of vibrational bands). They differ significantly between the two isomers.

Although the obtained IR-PD spectrum is rather noisy due to the difficulty of efficiently tagging the $C_{17}H_{11}^+$ cation with Ne, the comparison with the DFT spectra allows us to identify $PyrCH_2^+$ in these experiments. This assignment is based on at least 5 bands as listed in Table 1. There is no evidence for characteristic signatures of $PyrC_7^+$, but the low signal-to-noise ratio of the spectrum combined with the expected lower band intensities of $PyrC_7^+$ compared to $PyrCH_2^+$ (cf. Table 1) are not in favour of detecting this ion. In the case of the IRMPD spectrum, we also observe three bands that could be attributed to $PyrCH_2^+$. This conclusion is however challenged by the fact that the band measured at 1615 cm^{-1} in the PD experiments, which is the strongest in the theoretical spectrum of $PyrCH_2^+$, has no counterpart in the IRMPD spectrum. The band at about 1530 cm^{-1} is also missing. On the other hand, none of the predicted bands of $PyrC_7^+$ are observed in our IRMPD spectrum, which raises the question of the species that are traced by this latter spectrum.

It is interesting to compare our results with previous IRMPD spectra recorded on substituted benzylium (Bz^+) and tropylium (Tr^+) cations. Zins et al. [24] compared the IRMPD spectrum of the tert-butyl derivative of $C_7H_7^+$ with B3LYP calculations using the same scaling factor of 0.975 as in our work. They concluded that only Bz^+ can be observed. The characteristic band of the Tr^+ isomer at 1506 cm^{-1} was not observed but the authors argued that this is a sensitivity matter, considering that the computed absorption intensity of Tr^+ is a factor of $\sim$10 weaker than that of the strongest band of Bz^+. The IRMPD spectra of methyl-substituted species were recorded by Chiavarino et al. [25], showing that the major band of Bz^+ and Tr^+ species falls at 1600 and 1480 cm^{-1}, respectively. Finally, Morsa et al. [26] were able to produce preferentially the derivatives of Bz^+ and Tr^+ isomers of the $C_{11}H_{15}^+$ ion by tuning the activation regime of the precursor ion. The major bands of Bz^+ and Tr^+ derivatives were recorded in the IRMPD spectra at 1615 and 1425 cm^{-1}, respectively. All the above studies show that Bz^+ has a characteristic IR band at $\sim$ 1600 cm^{-1}, whereas a band is expected at $\sim$ 1500 cm^{-1} for Tr^+ species. Although our species are significantly different from these previously studied systems, their calculated IR spectra also carry these characteristic features, which are neither present in the spectrum of the regular neutral pyrene nor cationic pyrene (cf. Figure S5 in the SI). This can be understood if one considers the change in charge distribution from $C_{16}H_{10}^+$ to $PyrCH_2^+$ and $PyrC_7^+$ (see Mulliken charge distribution on Figure S4 in the SI) that leads to a dipole moment of 1.29 D for both isomers, in the XY plane following the orientation reported in Figure 1 (more specifically along the Y axis for $PyrC_7^+$). This is expected to lead to an enhancement of the IR intensity for the modes whose projection in the direction

of the dipole moment is significant, which is the case for some $\delta_{CH} + \nu_{CC}$ modes (in plane C-H bend and C-C stretch) such as those reported for instance on Figure S2 in the SI for $PyrC_7^+$ and on Figure S3 (e)-(f) in the SI for $PyrCH_2^+$.

Table 1: Experimental mid-IR band positions recorded for $C_{17}H_{11}^+$ and calculated positions for $PyrCH_2^+$ and $PyrC_7^+$ isomers (see Figure 2) obtained in the present work. The intensities corresponding to the maximum of the convoluted spectra are also reported.

Experiment		Calculations	
ν (cm^{-1}) IR-PD	ν (cm^{-1}) IRMPD	ν (cm^{-1}) DFT-B3LYP	Inten. ($km \cdot mol^{-1}$) DFT-B3LYP
		$PyrCH_2^+$	
1240(25)	1223(21)	1236	117
1376(9)	1362(23)	1376	144
1529(12)	–	1535	92
1570(21)	1568(26)	1574	154
1615(16)	–	1615*	407
		$PyrC_7^+$	
–	–	1212	148
–	–	1496	274

Note: Consult SI for the visualisation of modes. * – mode used to determine the scaling factor.

3.2. Dissociation dynamics

In order to shed more light on the measured IRMPD spectrum, we report in the following further insights into the dissociation dynamics of $C_{17}H_{11}^+$ ions. Dissociation rates, branching ratios and structures of the products and reaction intermediates were obtained from MD/SCC-DFTB simulations following the procedure detailed in Section 2.2 and starting from the two isomers $PyrCH_2^+$ and $PyrC_7^+$. The branching ratios and dissociation rates are determined at 24 and 19 eV (cf. Figure 3). The major fragment for both isomers corresponds to the loss of C_2H_2, H loss being second, but much lower. At both calculated energies, the dissociation of $PyrC_7^+$ is found to be slightly more efficient than that of $PyrCH_2^+$. We compared these results with calculations on the regular pyrene cation (cf. Figure S6 in the SI). For this ion, we know from comparison with photo-absorption experiments [27] that our calculations overestimate the contribution of the C_2H_2 channel and this challenging issue is currently under investigation. Still the C_2H_2/H fragmentation branching ratio is found to be larger for both isomers of $C_{17}H_{11}^+$ than for cationic pyrene. This indicates that C_2H_2 is a major fragmentation channel for $C_{17}H_{11}^+$ ions, which is also shown by our experimental results (cf. Table S1 in the SI) and a previous study [2].

From our simulations at 19 eV, we could get insights into the product structures and possible dissociation mechanisms. Some snapshots of simulations that

we estimated to be representative are reported in Figure 4 and in Figure S7 in the SI for both $PyrCH_2^+$ and $PyrC_7^+$. We found that a common structure for the dissociation product is the presence of a five-membered ring as earlier suggested [2]. The other noticeable product has undergone ring opening to form an acetylene terminal group. This terminal structure was also observed as the final product in several simulations for both isomers. It is presented in the case of $PyrCH_2^+$ in Figure S7 (a) in the SI.

All paths were found to involve H migrations, leading to the formation of quite long time scale intermediates. H migration also leads to the formation of sp^3 carbon atoms and weakening of the CC bond. In the case of $PyrCH_2^+$, one can notice the formation of a terminal -CH-CH_2 vinylidene function, which often appears as a long time intermediate in the simulations (cf. Figure 4 (a)). On the other example reported in Figure S7 (a) in the SI, we see that isomerisation into the tropylium-like isomer occurs following a mechanism invoked in Rapacioli et al. [3] (out of plane deformation of the PAH, CH_2 insertion and H migration). In the case of $PyrC_7^+$, one can observe the direct formation of a 5-membered ring (through a [5+4] intermediate, see first structure at the bottom of Figure 4 (b)) from the 7-membered cycle, followed by C_2H_2 loss. In the other selected path in Figure S7 (b) in the SI, one can see the variety of possible isomerisation reactions involving H migration, external ring opening and formation of acetylene terminal groups and five-membered rings. Interestingly, only the tropylium cycle in $PyrC_7^+$ and the C_6-CH_2 part of $PyrCH_2^+$ are altered, showing their enhanced fragility with respect to the rest of the carbon skeleton.

Overall, the results of these simulations can help us to rationalise the IRMPD spectrum. The simulations suggest a lower but comparable internal energy to dissociate $PyrCH_2^+$ and $PyrC_7^+$ as well as the pyrene cation. The dissociation threshold for the pyrene cation has been observed to be around 9 eV in other ion trap experiments using synchrotron radiation [28], corresponding to a micro-canonical temperature of 2200 K. We can therefore use this value as a first estimate of the internal energy required to dissociate $C_{17}H_{11}^+$. With this amount of internal energy, the system will be able to overcome the $PyrCH_2^+$ to $PyrC_7^+$ isomerisation barrier of $3.5 - 4.0$ eV [3]. Our simulations also suggest that the heated molecular ion can experience many isomeric forms on its way to dissociation involving not only the two lowest-energy isomers but also higher-energy ones. For IRMPD to occur, the irradiated ion should absorb continuously the IR laser irradiation to reach high enough internal energy/ temperature to dissociate. Isomerisation will affect the IR absorption spectrum. Figure S8 of the SI aims at illustrating this effect by mixing the harmonic spectrum of $PyrCH_2^+$ with those of the 3 isomers involved in the calculated dissociation path presented in Figure 4, panel (a). Although this spectrum cannot be compared directly to the IRMPD spectrum, it shows the spectral ranges with higher global absorption cross-section for the mixture of isomers. These spectral ranges are likely to have higher heating efficiency upon laser irradiation and therefore a higher IRMPD signal. Although this constructed global spectrum shows 3 comparably intense bands, it still does not explain the missing 1615 cm^{-1} band in the experimental IRMPD spectrum. Anharmonicity is another effect that can affect the IR

spectrum. Rapacioli et al. [3] calculated the IR spectra of $PyrCH_2^+$ and $PyrC_7^+$ as a function of temperature up to 2000 K. The spectra exhibit significant band shifts and broadening with temperature. Hence, the recorded IRMPD spectrum is expected to reflect the net efficiency of heating the ion while the absorption IR spectrum is modified by both isomerisation and anharmonic effects, making its interpretation very tricky. The impact of isomerisation during the IRMPD process has been previously discussed in the case of $C_7H_9^+$ [29]. We note that this issue has not been reported in the IRMPD studies on substituted benzylium (Bz^+) and tropylium (Tr^+) cations that are described in the previous section. The reason is that, for these systems, the involved dissociation energies were much lower making complex isomerisation pathways less competitive.

4. Conclusion

In summary, this work demonstrates the benefit of the combination of a widely tunable IR laser source (FELIX) with cold ions prepared in a 22-pole ion trap in probing the role of isomerisation in the photophysics of PAHs. In the specific case of $C_{17}H_{11}^+$, we showed that the IRMPD spectrum is difficult to analyse and can only bring limited information. This spectrum lacks the characteristic band around 1600 cm^{-1}, which has been observed in previous IRMPD spectra of benzylium-type species. Possible reasons include anharmonic effects and isomerization while heating the trapped ions, as suggested by molecular dynamics simulations. Further experimental work either on the anharmonic spectra or on the dissociation dynamics of $PyrCH_2^+$ would help to solve this issue. On the opposite, a clear relation between the one photon absorption bands of the IR-PD experiment and DFT predictions unravels the presence of the $PyrCH_2^+$ isomer in our experimental conditions. The $PyrC_7^+$ isomer was not observed due to the limited signal-to-noise ratio. Thus, the presence of this isomer at formation cannot be excluded.

Acknowledgments

We greatly appreciate the experimental support provided by the FELIX team. The research leading to this result is supported by the European Research Council under the European Union's Seventh Framework Programme ERC-2013-SyG, Grant Agreement n. 610256 NANOCOSMOS. We acknowledge support from the project CALIPSOplus under the Grant Agreement 730872 from the EU Framework Programme for Research and Innovation HORIZON 2020. S. B. and St. S. also acknowledge support from DFG SPP 1573 grant BR 4287/1-2. P. J. and the operation of the 22-pole ion trap were partially funded by the DFG via the Gerätezentrum "Cologne Center for Terahertz Spectroscopy" (DFG SCHL 341/15-1). G. W. is supported by the H2020-MSCA-ITN-2016 Program (EUROPAH project, G. A. 722346). A. S. would like to thank the computing facility CALMIP for generous allocation of computer resources. Finally, we thank the anonymous referees for helping improving this manuscript, in particular the analysis of the IRMPD spectrum.

Supplementary material

Supplementray material can be found online at: https://doi.org/10.1016/j.cplett.2018.03.028.

References

References

[1] A. Leger, L. D'Hendecourt, D. Defourneau, Proposed identification for the (common) carrier of the 4430A and 7565A DIBs., Astronomy & Astrophysics 293 (1995) L53–L56.

[2] D. L. Kokkin, A. Simon, C. Marshall, A. Bonnamy, C. Joblin, A Novel Approach to the Detection and Characterization of PAH Cations and PAH-Photoproducts, in: J. Cami, N. L. J. Cox (Eds.), The Diffuse Interstellar Bands, Vol. 297 of IAU Symposium, 2014, pp. 286–290. doi:10.1017/S1743921313016001.

[3] M. Rapacioli, A. Simon, C. C. M. Marshall, J. Cuny, D. Kokkin, F. Spiegelman, C. Joblin, Cationic methylener-pyrene isomers and isomerization pathways: Finite temperature theoretical studies, The Journal of Physical Chemistry A 119 (51) (2015) 12845–12854. doi:10.1021/acs.jpca.5b09494.

[4] J. Oomens, B. G. Sartakov, G. Meijer, G. von Helden, Gas-phase infrared multiple photon dissociation spectroscopy of mass-selected molecular ions, International Journal of Mass Spectrometry 254 (1) (2006) 1–19. doi:10.1016/j.ijms.2006.05.009.

[5] U. J. Lorenz, N. Solcà, J. Lemaire, P. Maître, O. Dopfer, Infrared spectra of isolated protonated polycyclic aromatic hydrocarbons: Protonated naphthalene, Angewandte Chemie International Edition 46 (35) (2007) 6714–6716. doi:10.1002/anie.200701838.

[6] P. Parneix, M. Basire, F. Calvo, Accurate modeling of infrared multiple photon dissociation spectra: The dynamical role of anharmonicities, The Journal of Physical Chemistry A 117 (19) (2013) 3954–3959. doi:10.1021/jp402459f.

[7] P. Jusko, S. Brünken, O. Asvany, S. Thorwirth, A. Stoffels, B. Redlich, L. van der Meer, J. Oomens, S. Schlemmer, Felion: Cryogenic 22 pole trap at the felix facility, In prep.

[8] D. Oepts, A. F. G. van der Meer, P. W. van Amersfoort, The Free-Electron-Laser user facility FELIX, Infrared Physics and Technology 36 (1995) 297–308. doi:10.1016/1350-4495(94)00074-U.

[9] H. Piest, G. von Helden, G. Meijer, Infrared Spectroscopy of Jet-cooled Cationic Polyaromatic Hydrocarbons: Naphthalene$^+$, The Astrophysical Journal 520 (1999) L75–L78. doi:10.1086/312143.

[10] J. H. Piest, J. Oomens, J. Bakker, G. von Helden, G. Meijer, Vibrational spectroscopy of gas-phase neutral and cationic phenanthrene in their electronic groundstates, Spectrochimica Acta Part A: Molecular and Biomolecular Spectroscopy 57 (4) (2001) 717–735. doi:10.1016/S1386-1425(00)00439-X.

[11] M. Brümmer, C. Kaposta, G. Santambrogio, K. R. Asmis, Formation and photodepletion of cluster ion-messenger atom complexes in a cold ion trap: Infrared spectroscopy of VO^+, VO_2^+, and VO_3^+, J. Chem. Phys. 119 (24) (2003) 12700–12703. doi:10.1063/1.1634254.

[12] J. Jašík, J. Žabka, J. Roithová, D. Gerlich, Infrared spectroscopy of trapped molecular dications below 4 K, Int. J. Mass. Spectrom. 354 (SI) (2013) 204–210. doi:10.1016/j.ijms.2013.06.007.

[13] D. Gerlich, Inhomogeneous RF fields: A versatile Tool for the Study of processes with Slow Ions, in: C.-Y. Ng, M. Baer (Eds.), Adv. Chem. Phys.: State-Selected and State-to-State Ion-Molecule Reaction Dynamics, Vol. LXXXII, Wiley, New York, 1992, pp. 1–176.

[14] K. Kharnaior, M. Devi, R. Duncan Lyngdoh, Generation of $C_7H_7^+$ cations with isomerization reactions, Computational and Theoretical Chemistry 1091 (2016) 150–164. doi:10.1016/j.comptc.2016.07.018.

[15] A. D. Becke, Density-functional thermochemistry. iii. the role of exact exchange, J. Chem. Phys. 98 (7) (1993) 5648–5652. doi:10.1063/1.464913.

[16] M. J. Frisch, J. A. Pople, J. S. Binkley, Self-consistent molecular-orbital methods. 25. suppementary functions for gaussian-basis sets, J. Chem. Phys. 80 (7) (1984) 3265–3269. doi:10.1063/1.447079.

[17] M. J. Frisch, G. W. Trucks, H. B. Schlegel, G. E. Scuseria, M. A. Robb, J. R. Cheeseman, G. Scalmani, V. Barone, B. Mennucci, G. A. Petersson, H. Nakatsuji, M. Caricato, X. Li, H. P. Hratchian, A. F. Izmaylov, J. Bloino, G. Zheng, J. L. Sonnenberg, M. Hada, M. Ehara, K. Toyota, R. Fukuda, J. Hasegawa, M. Ishida, T. Nakajima, Y. Honda, O. Kitao, H. Nakai, T. Vreven, J. A. Montgomery, Jr., J. E. Peralta, F. Ogliaro, M. Bearpark, J. J. Heyd, E. Brothers, K. N. Kudin, V. N. Staroverov, R. Kobayashi, J. Normand, K. Raghavachari, A. Rendell, J. C. Burant, S. S. Iyengar, J. Tomasi, M. Cossi, N. Rega, J. M. Millam, M. Klene, J. E. Knox, J. B. Cross, V. Bakken, C. Adamo, J. Jaramillo, R. Gomperts, R. E. Stratmann, O. Yazyev, A. J. Austin, R. Cammi, C. Pomelli, J. W. Ochterski, R. L. Martin, K. Morokuma, V. G. Zakrzewski, G. A. Voth, P. Salvador, J. J. Dannenberg, S. Dapprich, A. D. Daniels, Ö. Farkas, J. B. Foresman,

J. V. Ortiz, J. Cioslowski, D. J. Fox, Gaussian 09, Revision D.01, Gaussian Inc., Wallingford CT, 2016.

[18] A. Simon, M. Rapacioli, Chemical Modelling, Vol. 14, Royal Society of Chemistry, 2018, Ch. Energetic processing of PAHs: isomerisation and dissociation, pp. 195–216.

[19] G. Trinquier, A. Simon, M. Rapacioli, F. X. Gadéa, Pah chemistry at eV internal energies. 1. H-shifted isomers, Molecular Astrophysics 7 (2017) 27–36. doi:10.1016/j.molap.2017.02.001.

[20] G. Trinquier, A. Simon, M. Rapacioli, F. X. Gadéa, Pah chemistry at eV internal energies. 2. ring alteration and dissociation, Molecular Astrophysics 7 (2017) 37–59. doi:10.1016/j.molap.2017.02.002.

[21] M. Elstner, D. Porezag, G. Jungnickel, J. Elsner, M. Haugk, T. Frauenheim, S. Suhai, G. Seifert, Self-consistent-charge density-functional tight-binding method for simulations of complex materials properties, Phys. Rev. B 58 (11) (1998) 7260–7268. doi:10.1103/PhysRevB.58.7260.

[22] A. Simon, M. Rapacioli, G. Rouaut, G. Trinquier, F. X. Gadéa, Dissociation of polycyclic aromatic hydrocarbons: molecular dynamics studies, Philosophical Transactions of the Royal Society of London A: Mathematical, Physical and Engineering Sciences 375 (2092). doi:10.1098/rsta.2016.0195.

[23] T. Heine, M. Rapacioli, S. Patchkovskii, J. Frenzel, A. Koster, P. Calaminici, H. A. Duarte, S. Escalante, R. Flores-Moreno, A. Goursot, J. Reveles, D. Salahub, A. Vela, deMonNano, http://demon-nano.ups-tlse.fr/.

[24] E.-L. Zins, C. Pepe, D. Schröder, Methylene-transfer reactions of benzylium/tropylium ions with neutral toluene studied by means of ion-trap mass spectrometry, Faraday Discuss. 145 (2010) 157–169. doi:10.1039/B907236E.

[25] B. Chiavarino, M. E. Crestoni, O. Dopfer, P. Maitre, S. Fornarini, Benzylium versus tropylium ion dichotomy: Vibrational spectroscopy of gaseous $C_8H_9^+$ ions, Angewandte Chemie International Edition 51 (20) (2012) 4947–4949. doi:10.1002/anie.201200558.

[26] D. Morsa, V. Gabelica, F. Rosu, J. Oomens, E. De Pauw, Dissociation pathways of benzylpyridinium "thermometer" ions depend on the activation regime: An irmpd spectroscopy study, The Journal of Physical Chemistry Letters 5 (21) (2014) 3787–3791. doi:10.1021/jz501903b.

[27] B. West, F. Useli-Bacchitta, H. Sabbah, V. Blanchet, A. Bodi, P. M. Mayer, C. Joblin, Photodissociation of pyrene cations: Structure and energetics from $C_{16}H_{10}^+$ to C_{14}^+ and almost everything in between, The Journal of Physical Chemistry A 118 (36) (2014) 7824–7831. doi:10.1021/jp506420u.

[28] J. Zhen, S. Rodriguez Castillo, C. Joblin, G. Mulas, H. Sabbah, A. Giuliani, L. Nahon, S. Martin, J.-P. Champeaux, P. M. Mayer, VUV Photoprocessing of PAH Cations: Quantitative Study on the Ionization versus Fragmentation Processes, The Astrophysical Journal 822 (2016) 113. doi:10.3847/0004-637X/822/2/113.

[29] D. Schröder, H. Schwarz, P. Milko, J. Roithová, Dissociation routes of protonated toluene probed by infrared spectroscopy in the gas phase, The Journal of Physical Chemistry A 110 (27) (2006) 8346–8353. doi:10.1021/jp056962f.

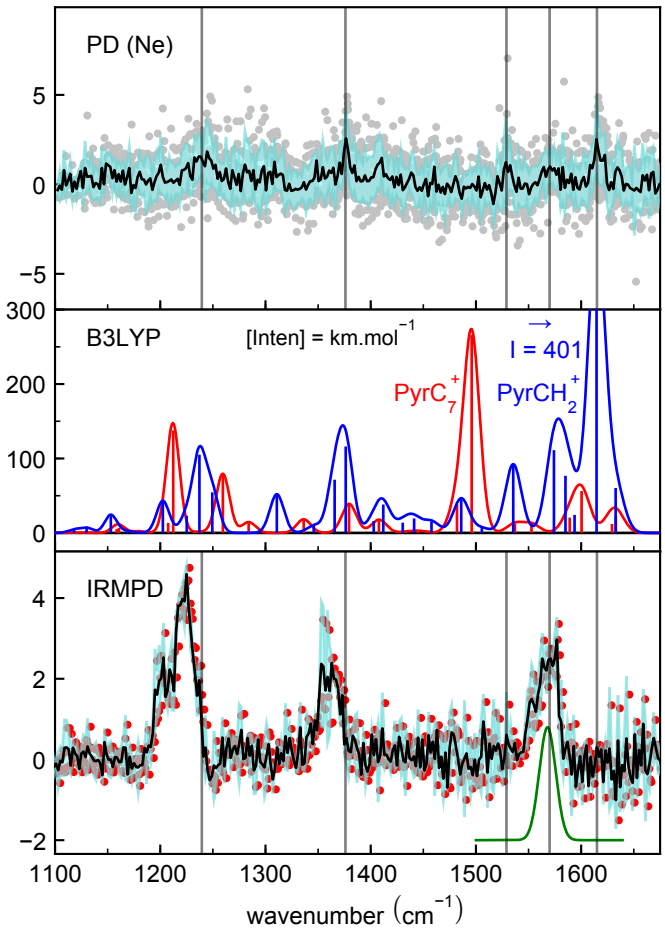

Figure 2: IR spectrum of $C_{17}H_{11}^+$ ($m/z = 215$). Top panel – IR pre-dissociation spectrum of the molecular ion tagged with Ne. Middle panel – stick spectrum corresponding to the scaled DFT harmonic spectra for the two isomers $PyrCH_2^+$ (blue) and $PyrC_7^+$ (red) with intensities in km.mol^{-1}. Convoluted spectra with $\sigma = 0.5\%$ BW are provided for comparison with the experiment. Bottom panel – IR multi-photon dissociation spectrum obtained by recording the fragment at $m/z = 189$ (loss of C_2H_2). Green line represents the approximate laser line profile. For experimental spectra, intensities are in arbitrary units and vertical lines correspond to the identified bands in the PD spectrum. (cf. Table 1).

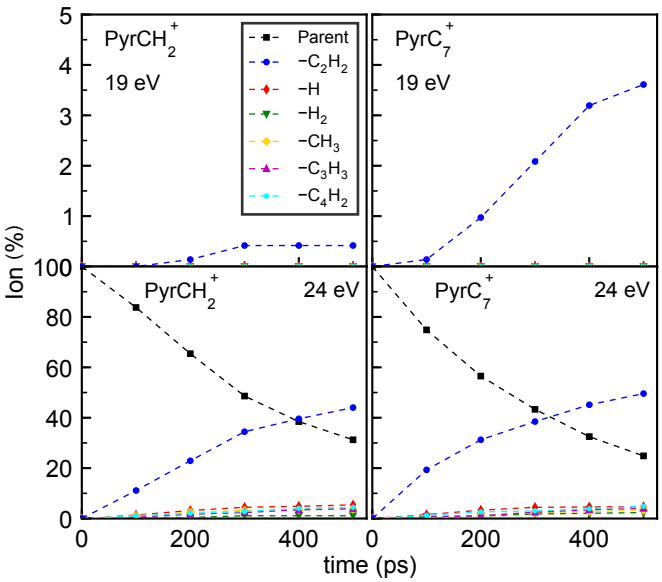

Figure 3: Dissociation of $PyrCH_2^+$ and $PyrC_7^+$: branching ratios as a function of time obtained from MD/SCC-DFTB simulations at 19 and 24 eV. The lines between data points are drawn to guide the eyes.

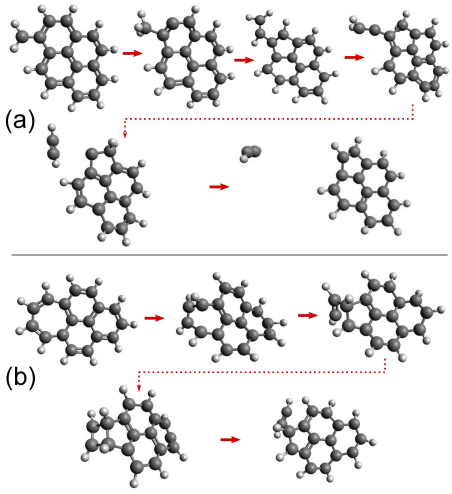

Figure 4: Examples of dissociation paths : snapshots extracted from 500 ps MD/SCC-DFTB trajectories run at 19 eV for $PyrCH_2^+$ (a) and $PyrC_7^+$ (b).